Received: 28 February 2022 | Revised: 25 April 2022 | Accepted: 17 May 2022

DOI: 10.1111/jfbc.14279

Journal of Food Biochemistry WILEY

ORIGINAL ARTICLE

Structural and inhibitory effects of fulvic and humic acids against tyrosinase

Negar Taherkhani[1] | Azadeh Hekmat[1] | Hossein Piri[2] | Kamahldin Haghbeen[3]

[1]Department of Biology, Science and Research Branch, Islamic Azad University, Tehran, Iran

[2]Cellular and Molecular Research Center, Research Institute for Prevention of Non-Communicable Disease, Qazvin University of Medical Sciences, Qazvin, Iran

[3]Biochemistry and Biophysics Department, National Institute for Genetic Engineering and Biotechnology, Tehran, Iran

Correspondence
Azadeh Hekmat, Department of Biology, Science and Research Branch, Islamic Azad University, Tehran, Iran.
Email: hekmat@ut.ac.ir

Abstract

Inhibition of tyrosinase activity can control fruit browning and preserve the flavor and nutritional value of food. The impacts of fulvic acid (FA) and humic acid (HA) on tyrosinase activity were investigated utilizing circular dichroism (CD) and fluorescence spectroscopy, molecular docking (MD), and molecular dynamics simulations. HA and FA demonstrated a mixed type of inhibition with K_i 2.02 and 5.2 μM, respectively. The thermodynamic parameters displayed that the hydrogen bond and hydrophobic force play a major role in the FA-tyrosinase and HA-tyrosinase interaction, respectively. Fluorescence experiments demonstrated changes in tyrosinase tertiary structures. HA could not destroy the tyrosinase secondary structure significantly, however, FA has a significant influence on the tyrosinase secondary structure. The molecular dynamics findings demonstrated the minimal fluctuations and the lowest flexibility in the complex amino acids in the HA-tyrosinase and FA-tyrosinase interaction. Altogether, HA and FA could be utilized in food industries as an accessible natural source for tyrosinase inhibition.

Practical applications

Recently, the investigation of tyrosinase inhibitors from the biosphere for hindrance of undesired browning in the food industry has increased considerably. Mushroom tyrosinase is a suitable model for kinetic research owing to its availability as well as close conformational similarity to tyrosinase in a mammal. Natural sources and their effective compounds could have wonderful potential on tyrosinase activity and structure, thus, in this study, the interactions between tyrosinase and fulvic acid (FA) and Humic acid (HA) were investigated. Previously, it has been shown that HA and FA have antioxidant properties and they can improve the quality of food via retarding lipid oxidation. Altogether, further investigations are warranted to draw firm conclusions, HA and FA could be utilized in food industries not only as antioxidant agents but also as an accessible natural source for tyrosinase inhibition.

KEYWORDS
fulvic acid, humic acid, molecular docking (MD), spectroscopy, tyrosinase inhibition

1 | INTRODUCTION

Enzymes accelerate biochemical reactions in living organisms and play an important role in biological processes (Robinson, 2015). Tyrosinase (EC 1.14.18.1) is a bifunctional and glycosylated enzyme extensively distributed in plants, mammals, as well as prokaryotes. Tyrosinase possesses two activities in its catalytic cycle, that is, this copper-containing enzyme catalyzes oxidation and hydroxylation of diphenols and mono phenols, respectively (Gheibi et al., 2015; Nanok & Sansenya, 2020). Naturally, L-3,4-dihydroxyphenylalanine (L-DOPA), as well as L-tyrosine, are substrates of oxidase (diphenolase) and oxygenase (monophenolase) activities, respectively. Tyrosinase catalyzes the hydroxylation of tyrosine to form L-DOPA. Furthermore, it catalyzes L-DOPA to DOPA quinine. Subsequently, Quinones develop into melanins and other polyphenolic compounds chemically (Athipornchai et al., 2021). Tyrosinase is utilized in the fine chemical industry, environmental applications, food, and medicine. It is the major enzyme that is accountable for the browning of vegetables, fungi, and fruits as well as melanogenesis in mammals (Zhou et al., 2016). In the food industry, the activity of tyrosinase and subsequent oxidation of phenols to form melanin is undesirable which diminishes the flavor and nutritional value of food (Li et al., 2021). Therefore, the prevention of tyrosinase activity leads scientists to design inhibitors of tyrosinase.

Owing to the crucial role of tyrosinase, numerous studies have been performed on the detection of tyrosinase inhibitors from various synthetic or natural sources (Zolghadri et al., 2019). For example, the antityrosinase activity of santalin, a natural red constituent in *Pterocarpus santalinus*, has been reported (Hridya et al., 2016). Anantharaman et al. reported that crocin, norbixin, and bixin (apocarotenoids compounds) have an inhibitory effect against tyrosinase activity. They found that the inhibition of tyrosinase activity by crocin and norbixin was of the mixed competitive type. However, bixin inhibited tyrosinase activity by a mixed-type mechanism (Anantharaman et al., 2016). The inhibitory impacts of aromatic thiosemicarbazones on tyrosinase were investigated also investigated by Hałdys et al. who exhibited that there is an association between the structure of examined molecules and their inhibitory activity (Hałdys et al., 2018). Lots of kinetic research have been performed on tyrosinase in mushroom owing to the complexities of working with tyrosinase from human along with the behavior similarities among tyrosinase in mammal and mushroom tyrosinase (Hassani et al., 2018). Mushroom tyrosinase, with a molecular weight of about 120 kDa, is an asymmetric tetramer (H2L2). Both heavier subunits of active mushroom tyrosinase are ~43 kDa and carry a binuclear Cu active site, whereas the lighter subunits of mushroom tyrosinase lack an active site (Hassani et al., 2018).

Humic substances (HS), one of the valuable matters of the biosphere, are responsible for several chemical and physical processes in soil. HS is produced by the organization of high-molecular-mass matters from animal origin, vegetative, as well as microbiological. They are a structurally particularized element of soil organic matter. Humic compounds are categorized into three categories: fulvic acids (FAs), humin, as well as humic acids (HAs) (Peña-Méndez et al., 2005; Tan, 2014). Humin is water-insoluble, HA compounds in the free form can be dissolved in water in basic and neutral solutions, whereas FA compounds in the free form can be dissolved in water at all values of pH. Commonly, HAs are larger than FAs which in turn include less carbon and more oxygen than HAs (Albers et al., 2008; Christl et al., 2008). Humic substances have a chemically complex and amorphous structure with a polyelectrolyte nature. In HAs there are compounds with significant medicinal or pharmaceutical properties. Various studies have shown that Humic substances have detoxification, anti-inflammatory, anticancer, antiviral, anti-inflammatory and pro-inflammatory, antiaging, and antidiabetic properties (Bondareva & Kudryasheva, 2021; Jacob et al., 2019; van Rensburg, 2015). It is becoming even more apparent that FA substances have antibacterial, anti-inflammatory, antiwrinkle, as well as detoxification effects (Kinoshita et al., 2012; Wahyudi et al., 2010; You et al., 2021). FAs have less reversible redox sites (e.g., quinone moieties) and lower average molecular weight than HAs, however, HAs display more color and aromaticity than FAs (Li et al., 2016). The interaction of Humic compounds with lysozyme (Tan et al., 2008, 2009), Cry1Ab protein (Sander et al., 2012; Tomaszewski et al., 2012), and bovine serum albumin (BSA) (Guan et al., 2018) was investigated and the importance of hydrophobic as well as electrostatic interactions was indicated. The inhibitory effects of FAs and HAs against the glutathione peroxidase and superoxide dismutase activity were reported (Afifi, 2017).

Humic compounds are among the most broadly distributed organic materials in nature and their significance in soil sciences has been accepted for over150 years. Furthermore, humic substances are recommended as dietary supplements. Consistent with the collective indication of the molecular and biochemical impacts of humic compounds, these compounds could be robust candidates for inhibiting enzymes. Thus, in this study, owing to the impact of tyrosinase in the food industry and due to the fact that natural sources and their effective compounds could have wonderful potential on tyrosinase activity and structure, the interactions between tyrosinase and humic substances (HA and FA) were investigated. All information presented in this study could offer lead to the exploration of practical agents against tyrosinase activity in the food industries.

2 | MATERIALS AND METHODS

2.1 | Materials

Mushroom tyrosinase from *Agaricus bisporus* (lyophilized powder, 3600 U/mg, Product No. T3824), 3,4-dihydroxy-L-phenylalanin (L-DOPA), fulvic acid ($C_{14}H_{12}O_8$, powder, Product No. 25195, Figure 1a), and humic acid (powder, Product No. 53680, Figure 1b) were acquired from Sigma Co., St. Louis, MO, U.S.A. Na_2HPO_4 and NaH_2PO_4 were obtained from Merck Co., Germany. All trials were done in phosphate-buffered saline (PBS; pH 6.8; 10 mM). Buffer was prepared with double-distilled water by Barnstead Nanopure (ER = 18.3 MΩ).

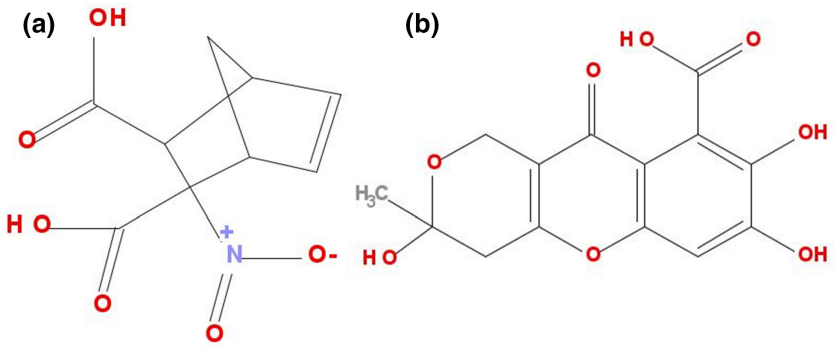

FIGURE 1 The structures of (a) humic acid and (b) fulvic acid.

2.2 | Enzyme assay and measurement of kinetic parameters

The spectrophotometric assay for the diphenolase activity of tyrosinase was examined based on the previous method with a slight alteration (Yang et al., 2016). L-DOPA is the substrate of tyrosinase that generates *o*-quinone that turns into dopachrome. The experimentally measurable velocity of the diphenolase activity can be examined by determining the accumulation of dopachrome, directly (Hassani et al., 2018). Therefore, rates of dopachrome formation were determined at λ_{max} =475 nm and ε = 3700 M^{-1} cm^{-1} in the initial 5 min by utilizing the UV-2100 Double Beam UV/Vis spectrophotometer (China). The reaction media is 1 ml in PBS (10 mM, pH 6.8). The final concentration of tyrosinase was 17 mg/ml. The enzymatic reactions were examined with a fresh stock solution of tyrosinase and substrate. The reaction was performed under constant temperatures of 27°C. Enzyme activity was measured by utilizing different fixed concentrations of L-DOPA (0.1, 0.5, 1, and 1.5 mM) in various concentrations of FA or HA (2, 6, 9, and 12 μM). Results are the averages of five measurements. Maximal velocity (V_m), Michaelis constant (K_m), and kinetic parameters of tyrosinase were evaluated utilizing Lineweaver-Burk plots.

2.3 | The intrinsic fluorescence measurements

The intrinsic fluorescence of tyrosinase in the presence and absence of fulvic acid or humic acid was performed via a spectrofluorometer (Varian Cary Eclipse, U.S.A) using a 1 cm quartz cell at 27 and 37°C. The excitation wavelength was 280 nm. In all cases, 10 nm emission and excitation slits were utilized. FA or HA (2, 6, 9, and 12 μM) were added to the tyrosinase solution (17 mg/ml), and fluorescence investigations were obtained. By adding portions of PBS, the concentration of tyrosinase and the sample volume were maintained constant. For inner filter impact correction affected by the emission and excitation signals attenuation generated from the quencher absorption, Equation 1 was applied (Hekmat et al., 2021):

$$F_{corr} = F_{obs} \cdot 10^{(Ab_{ex}+Ab_{em})/2}, \quad (1)$$

where Ab_{em}, Ab_{ex}, F_{obs}, and F_{corr} are the mixture absorption at emission as well as excitation wavelengths, the observed fluorescence intensity, and the corrected fluorescence intensity, respectively (Pashah et al., 2019).

2.4 | Circular dichroism (CD) measurements

The far UV-CD analysis was performed utilizing Aviv Circular Dichroism Spectrometer, Model 215, U.S.A, with a 0.2 nm resolution and 20 nm min^{-1} speed scanning at 27°C. By adding FA (12 μM) or HA (12 μM) to tyrosinase solution (17 mg/ml), the CD spectra were assessed in the wavelength range of 190–260 nm by means of a quartz cell and a path length of 1 mm. The CD spectra deconvolution software (CDNN, version 2.1) was applied to analyze the CD spectra.

2.5 | Molecular dynamics (MD) simulation

The X-ray crystal structure of the fulvic acid (entry code: 5359407) and humic acid (entry code: 90472028) were provided from NCBI PubChem Compound Database. The tyrosinase crystal structure (PDB ID: 2Y9X) was derived from RCSB Protein Data Bank (http://www.rcsb.org). To evaluate the permissible torsions for the ligand and distinguish the search space coordinates, the AutoDock Tools program (version 4.2.5.1) was utilized for preparing all the input files (Hanai et al., 2002). Subsequently, the docking process was accomplished via a grid size of 100×94×126 along the X, Y, and Z axes with 1 Å spacing. Then, the lowermost values of the binding energy of fulvic acid-tyrosinase and humic acid-tyrosinase were achieved. The best pose with promising binding free energy was chosen as the initial structure in the MD simulations.

The MD simulation procedure was performed utilizing the GROMACS program (version 4.5.4) and for all simulations, the CHARMM 36 force field was utilized (Lindahl et al., 2001). By transferable intermolecular potential with 3 points (TIP3P) water model, the tyrosinase, FA–tyrosinase, and HA-tyrosinase complexes were solvated in a cubic box with a 10 Å distance from the furthest atom of tyrosinase. To neutralize the solvent, chloride (Cl^-) and sodium (Na^+) ions were added to the system. Subsequently, 150 mM $CaCl_2$ and NaCl were added to the systems. Utilizing the steepest descent method, energy minimization was performed. To permit the equilibration of the systems, all solvents were balanced via 1 ns MD simulation in the

isothermal–isobaric (NPT) ensemble as well as 1 ns MD simulation in the canonical (NVT) ensemble utilizing position restraints on the tyrosinase heavy atoms. For fixing the temperature of the system at 300 K, the Nose–Hoover thermostat constant was applied. Besides, to keep the system pressure at 1 bar, the Parrinello–Rahman pressure coupling method was utilized. Last, for all equilibrated systems, the MD simulation process was performed twice with time steps of 2 fs for about 100 ns. Additionally, to study FA–tyrosinase and HA–tyrosinase interactions, RMSD (Root Mean Square Deviation) and RMSF (Root Mean Square Fluctuation) were measured utilizing GRO-MACS software through the simulation. Subsequently, to achieve the final PDB file of the MD simulation procedure, the Pymol software was utilized (Farasat et al., 2020; Gheibi et al., 2020).

2.6 | Statistical analysis

The data were recorded as mean ± standard deviation of the mean (n = 5). The ANOVA (one-way analysis of variance) was employed to evaluate the mean of different data sets.

3 | RESULTS AND DISCUSSION

3.1 | Inhibition types and constants of tyrosinase by HA and FA

Additions of both HA and FA in reaction mixtures of tyrosinase and L-DOPA at 27°C have indicated potent inhibitory impacts of these compounds. In order to understand the type of inhibitions, the kinetic parameters for tyrosinase were attained from Lineweaver–Burk doubles reciprocal plot (1/V vs. 1/[S]). Results showed that HA and FA had a dose-dependent inhibitory action against tyrosinase (Figure 2). Various straight lines intersected at the same point in the second quadrant, while K_m (Michaelis constant) increased and V_{max} (maximum velocity) reduced regularly after the addition of FA or HA with different concentrations, signifying that FA and HA were mixed-type inhibitors for tyrosinase (Yang et al., 2016). This type of inhibition revealed that HA and FA coupled on both the tyrosinase–L-DOPA adaptors and the free tyrosinase. Mixed inhibition is a common mode detected in the kinetics experiments on mushroom tyrosinase activities. Thymol analogs (Ashraf et al., 2015), brazilein (Hridya et al., 2015), D-(−)-arabinose (Liu et al., 2012), isorhamnetin (Yu et al., 2019), terephthalic acid (Yin, Si, Chen, et al., 2011), and santalin (Hridya et al., 2016), phthalic acid (Yin, Si, & Qian, 2011) are some examples of mixed type inhibitors of diphenolase activity.

The secondary replots of Y-intercept and slope vs. [HA] or [FA] were linear (insets of Figure 2), indicating that HA and FA may possess a single binding site on tyrosinase or the same group of binding sites. The inhibition constants (K_i), the interaction factor (α) for binding of HA and FA to the free tyrosinase, and the half-maximal inhibitory concentration (IC_{50}) were acquired from Equations 2–4 (Burlingham & Widlanski, 2003).

$$\text{Y} - \text{intercept} = \frac{1}{V_{max(app)}} = \frac{1}{V_{max}} + \frac{1}{\alpha K_i V_{max}}, \quad (2)$$

$$\text{slope} = \frac{K_m}{V_{max}} = \frac{K_m[\text{I}]}{K_i V_{max}}, \quad (3)$$

$$IC_{50} = \frac{[S] + K_m}{\frac{[S]}{\alpha K_i} + \frac{K_m}{K_i}}. \quad (4)$$

The IC_{50} of HA-tyrosinase and FA-tyrosinase interactions were determined to be 2.43 and 8.25 μM, respectively. Yang et al. (2016) reported that hollow nanoparticles restrained the L-DOPA oxidation with an IC_{50} of lower than 4.774 μM and they established that compared with other inhibitors, their selected ligands have more inhibitory effects. The reported IC_{50} values of Kojic acid analogs (well-known tyrosinase inhibitors) are in the range of 1.35–12.5 μM (Chen et al., 2016; Zolghadri et al., 2019). The values of K_i and α were 2.02 μM and 4.95 for HA-free tyrosinase binding and 5.2 μM and 3.51 for FA-free tyrosinase binding. The smaller the K_i value, the larger the binding affinity, as well as the smaller quantity of medication required to inhibit the enzyme activity. Thus, compared with other inhibitors (Uesugi et al., 2017; Zolghadri et al., 2019), FA and particularly HA showed significant inhibitory effects. The improved inhibitory activity for HA compared with FA could be attributable to the diverse compartments where the small molecular substrate and tyrosinase were positioned in.

3.2 | Steady-State fluorescence studies

The prominent inhibitory action of HA and FA vs. tyrosinase showed that these two inhibitors might directly combine with tyrosinase. The variations in the tertiary structure of tyrosinase after the addition of HA and FA were determined by fluorescence spectroscopy. To acquire information about the conformational alterations, tryptophan fluorescence has been evaluated as an intrinsic aromatic fluorophore in tyrosinase. The emission spectra of the tyrosinase with various concentrations of HA and FA at 27 and 37°C were demonstrated in Figure 3a–d. The intensity of tyrosinase diminished regularly with increasing concentrations of HA and FA, signifying that the intrinsic fluorescence of tyrosinase could be quenched by HA and FA intensively (Ashoka et al., 2006). This was possibly attributed to biomolecule binding, tyrosinase denaturation, or tyrosinase conformational modifications. It should be mentioned that tyrosinase does not undergo any gross structural alterations at these temperatures. There was no obvious shift at the $\lambda_{max,em}$ of tyrosinase fluorescence emission when the solutions of HA and FA were added which revealed the polarity of the microenvironment of tryptophan in tyrosinase was little influenced. Our obtained results are consistent with those of Yin et al. who have determined no obvious shift in the $\lambda_{max,em}$ of tryptophan after the addition of phthalic acid which inhibited tyrosinase in a mixed-type manner (Yin, Si, & Qian, 2011).

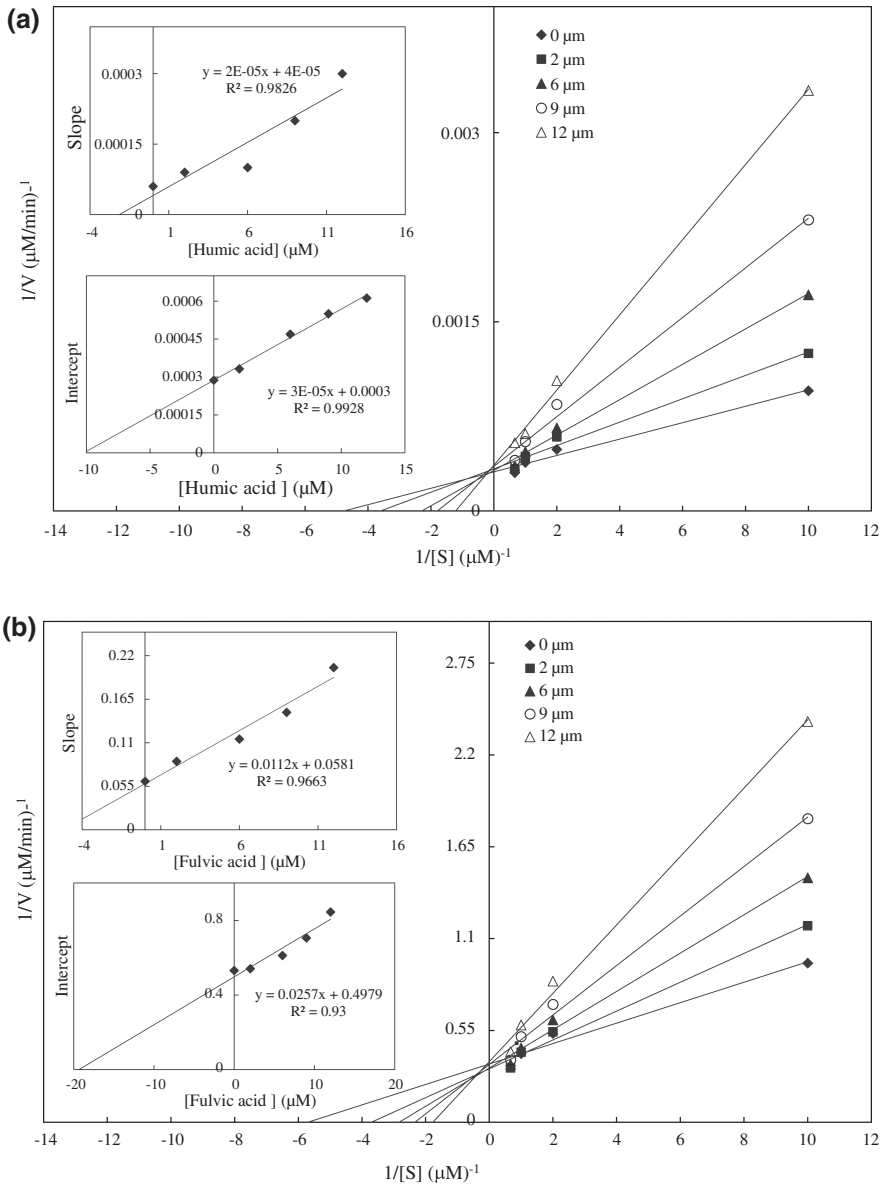

FIGURE 2 Lineweaver-Burk plots for tyrosinase inhibition in the presence of HA (a) and FA (b). Concentrations of HA and FA were 2, 6, 9, and 12 μM. The concentrations of L-DOPA were 0.1, 0.5, 1, as well as 1.5 μM. The insets signify the plot of the slope or the vertical intercepts vs. inhibitors concentrations. The lines were drawn utilizing linear least-squares fit.

3.3 | Mechanism of fluorescence quenching

Usually, fluorescence quenching is classified as static as well as dynamic quenching. To determine the tyrosinase binding mechanism to HA and FA, the fluorescence intensity data were evaluated through the classical Stern–Volmer equation (Equation 5) (Zhang et al., 2014).

$$\frac{F_0}{F} = 1 + K_{SV}[Q]. \quad (5)$$

In this equation, F, F_0 K_{sv}, and [Q] are the fluorescence intensity with a quencher (HA or FA), the fluorescence intensity without a quencher, the Stern–Volmer quenching constant, and the HA or FA concentrations, respectively. Applying Equation 5, the plots for F_0/F vs. [HA] or [FA] were drawn. As demonstrated in the insets of Figure 3e,f, the experimental Stern-Volmer plot for HA and FA displayed a positive deviation. Consequently, the mechanism of binding of HA and FA to tyrosinase was initiated mainly through the formation of the nonfluorescence complex (static quenching) (Hekmat et al., 2021).

Presuming that there were independent and equivalent binding groups in tyrosinase, the values of n (the number of binding sites), and K_A (the binding constant) were determined for HA-tyrosinase and FA-tyrosinase at both temperatures. Along with Equation 6 (Lu et al., 2016), K_A and n were calculated (Table 1).

$$\log\frac{F_0 - F}{F} = \log K_A + n\log[Q]. \quad (6)$$

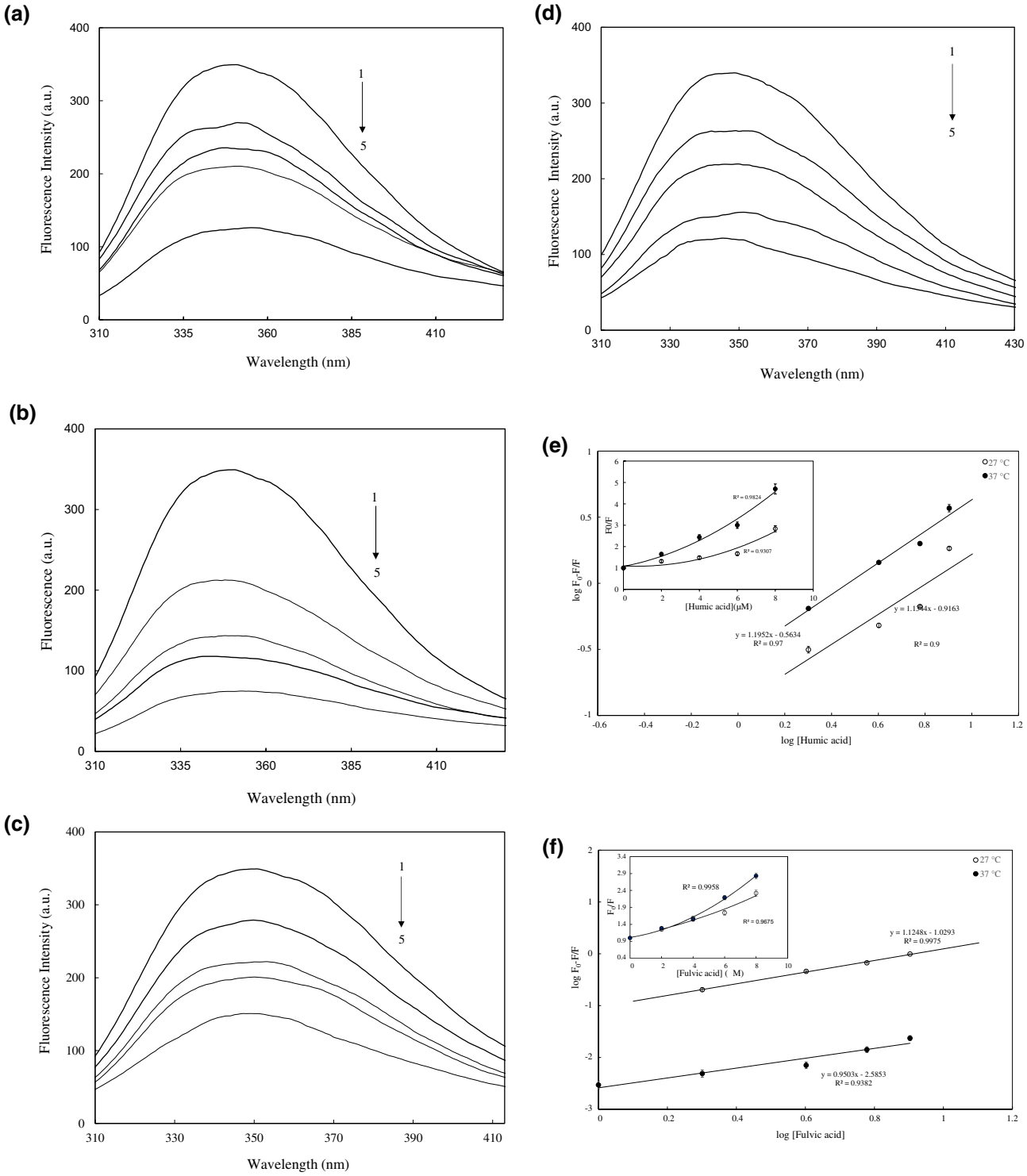

FIGURE 3 The fluorescence emission spectra of tyrosinase after adding various concentrations of HA at 27°C (a) and 37°C (b); and of FA at 27°C (c) and 37°C (d). The fluorescence emission of free tyrosinase (1), the fluorescence quenching with increasing concentrations of inhibitors (2–5). The modified stern-Volmer plot of tyrosinase in the presence of varying concentrations of HA (e) and FA (f). The inset indicates the classic stern–Volmer plot of tyrosinase in the presence of diverse concentrations of inhibitors. The data are attained from the means of three independent measurements ± SD.

The value of *n* is the reaction stoichiometric number, suggesting the amount of accessible binding sites on the surface of tyrosinase (Hekmat et al., 2022). From our analysis, the values of *n* at both temperatures were nearly equal to 1 suggesting that HA or FA could bind to tyrosinase, making a 1:1 adduct, that is, one molecule of HA or FA combined with one molecule of tyrosinase and that only one site in tyrosinase is reactive to HA or FA. This result proposes that the molecular population of a system in both temperatures contributes nearly equally

TABLE 1 Thermodynamic parameters and binding constants for FA-tyrosinase complex and HA-tyrosinase complex at two different temperatures

	T (°C)	n	K_A (M^{-1})	$\Delta G°$ ($kJ\,Mol^{-1}$)	$\Delta H°$ ($kJ\,Mol^{-1}$)	$\Delta S°$ ($J\,Mol^{-1}\,K^{-1}$)
FA-tyrosinase	27	1.2	9.36×10^4	−28.55	−277.08	−828.42
	37	0.9	2.6×10^3	−20.27		
HA-tyrosinase	27	1.1	1.21×10^5	−29.32	62.91	307.46
	37	1.2	2.73×10^5	−32.40		

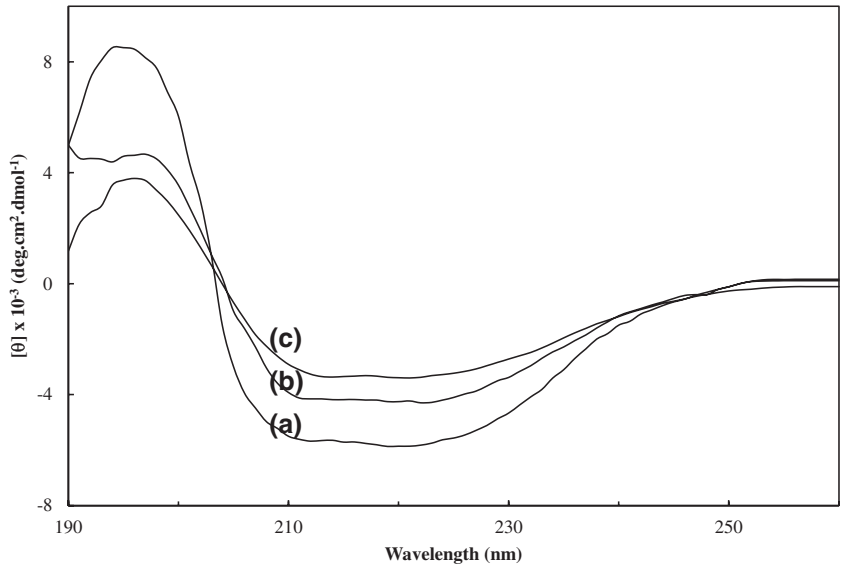

FIGURE 4 The far-UV CD spectra of tyrosinase in the absence (a) and presence of humic acid (b) and fulvic acid (c).

to molecular interactions in the formation of HA or FA complex with tyrosinase (Hekmat et al., 2022). K_A is an indication of the presence of binding sites in a biomacromolecule whose occupation relies on the small molecular substrate affinity to a receptor (Hekmat et al., 2022). The higher value of K_A for HA than that of FA implied that HA had a greater binding capability with tyrosinase than FA. Thus, HA may prevent the binding of L-DOPA to active sites. This result is correlate with the findings achieved from Lineweaver-Burk plots. According to Table 1, raising the temperature may cause some conformational alterations in the structure of tyrosinase which enables the binding of HA to tyrosinase molecule (enhancing "K_A"). This phenomenon displays the role of hydrophobic forces in the HA-tyrosinase binding process due to the fact that the temperature can improve the strength of hydrophobic interactions in an aqueous medium. In contrast, if the binding process is mainly commenced by hydrogen bonding and/or electrostatic interactions, reducing the K_A value is anticipated to be detected (Hekmat et al., 2021). Thus, the hydrogen bond performs the main role in the binding of FA with tyrosinase. However, the hydrophobic force presents a major role in the binding of HA with tyrosinase.

3.4 | The binding force determination

Utilizing K_A, the absolute temperature (T), and the universal gas constant (R) the standard Gibbs free energy change ($\Delta G°$) can be determined from Equation 7 (Ahmad et al., 2011; Hekmat & Saboury, 2019):

$$\Delta G^{\circ} = -RT\ln K \tag{7}$$

The magnitudes of $\Delta G°$ were calculated at both temperatures for HA and FA (Table 1). The negative values of $\Delta G°$ indicate that the binding of HA or FA to tyrosinase was spontaneous (Rahman et al., 2019). Employing Van't Hoff equation (Equation 8), the values of entropy change ($\Delta S°$) and enthalpy change ($\Delta H°$) were determined (Hekmat & Saboury, 2019).

$$\ln K_A = \frac{-\Delta H^{\circ}}{R}\frac{1}{T} + \frac{\Delta S^{\circ}}{R}. \tag{8}$$

Consistent with the literature, if $\Delta S°<0$, $\Delta H°<0$, the hydrogen bond performs a main impact in the interaction and if $\Delta S°>0$, $\Delta H°>0$, the main force is hydrophobic interaction (Hekmat & Saboury, 2019). Accordingly, in HA–tyrosinase interaction, the positive values of $\Delta S°$ and $\Delta H°$ values show that the hydrophobic force performs a principal role (Hekmat & Saboury, 2019; Moosavi-Movahedi et al., 2004). In FA–tyrosinase interaction, the negative $\Delta S°$ and $\Delta H°$ values show that the hydrogen bond performs the main effect.

3.5 | Secondary structure analysis

The CD spectra of tyrosinase demonstrated two negative maxima at ~222 nm and ~212 nm (Figure 4), which demonstrated the n–π^* transition as well as the π–π^* transition of the α-helical structure of

tyrosinase (Yang et al., 2016). After the addition of HA or FA to the tyrosinase solution, the CD signal of tyrosinase diminished without a significant band shift, indicating the content decline of the α-helical structure. As shown in Table 2, the native form of tyrosinase had 49.7% α-helixes, 11.3% β-sheets, 19.8% β-turns, and 19.2% unordered coils. After the addition of HA and FA, the α-helix diminished by 46.5% and 44.3%, respectively. A comparison of HA and FA results suggests that FA affects more instability in enzyme structure than HA. The outcome proposed that HA or FA combined with the amino acid residues of tyrosinase disturbed the hydrogen bonding formation and induced variations in the conformation of tyrosinase (Ding et al., 2019). It should be mentioned that till now the correlation between the catalytic activity of tyrosinase and its secondary structure is unclear. In earlier literature, the interaction of small molecules with tyrosinase can abolish the hydrogen networks and initiate the structural variations, which eventually cause the reduction of tyrosinase activity (Anantharaman et al., 2016; Fan et al., 2017; Yang et al., 2016; Yu et al., 2019). However, in some literature, inhibitors cannot change the secondary structure of tyrosinase even though they inhibit tyrosinase activity with good efficacy (Mu et al., 2013; Yu et al., 2019). Therefore, we can conclude that HA could not disorganize the secondary structures of tyrosinase significantly, however, it has a major impact on tyrosinase activity. On the contrary, FA has a significant impact on the secondary structure of tyrosinase activity and therefore can inhibit tyrosinase activity.

TABLE 2 Content of the secondary structure of tyrosinase in the absence and presence of fulvic acid and humic acid at 27°C

	α-Helix (%)	β-Sheet (%)	β-Turn (%)	Rndom coil (%)
Free tyrosinase	49.7	11.3	19.8	19.2
HA-tyrosinase	46.5	12.2	20.1	21.2
FA-tyrosinase	44.3	12.4	21.5	21.8

3.6 | Molecular docking (MD) and molecular dynamics results

MD was performed to evaluate the binding of HA or FA with specific binding sites on tyrosinase. The docking results revealed that HA and FA can bind to the active site of tyrosinase with the lowest binding energies of −4.2 and −6.4 kcal/mol, respectively. It must be mentioned that as a general rule, the lowest binding free energy of the enzyme–inhibitor binding was utilized as models for MD simulation (Farasat et al., 2020; Jamali et al., 2019). The 2D illustrations of tyrosinase–inhibitor complexes of MD simulation are displayed in Figure 5. This figure displays the residues of tyrosinase that participated in H-bonds and the length of them with a green dashed line. Nonligand residues that participated in hydrophobic forces are

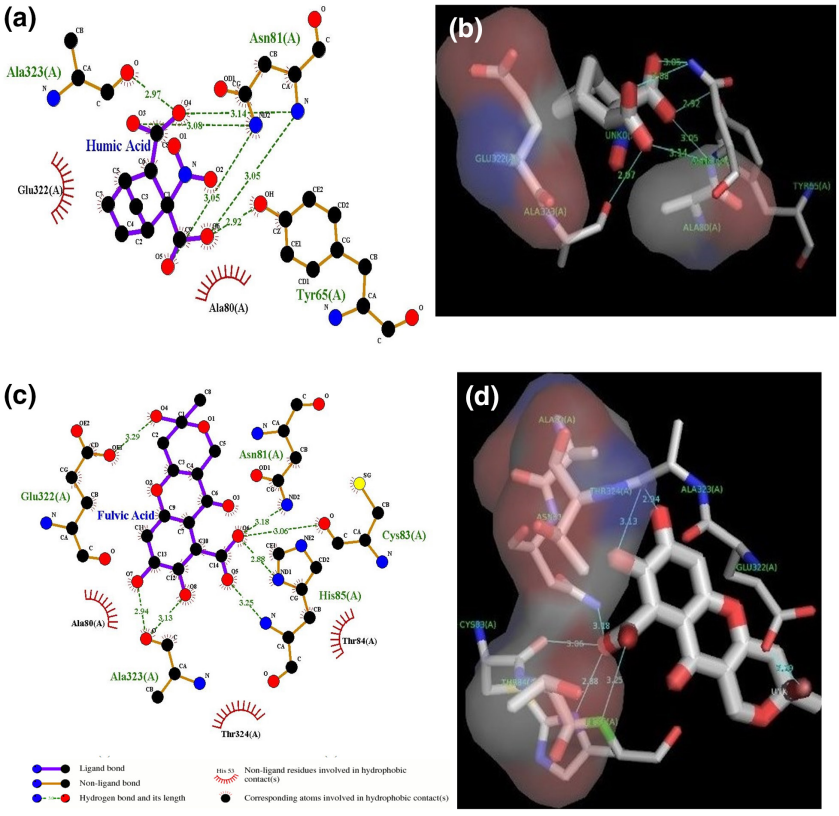

FIGURE 5 Molecular docking model of tyrosinase and HA and FA. The 2D projection of HA-tyrosinase (a) and FA-tyrosinase (b) docking model. The figure was created in LigPlot. The 3D map of HA (c) and FA (d) docking in the tyrosinase activity center.

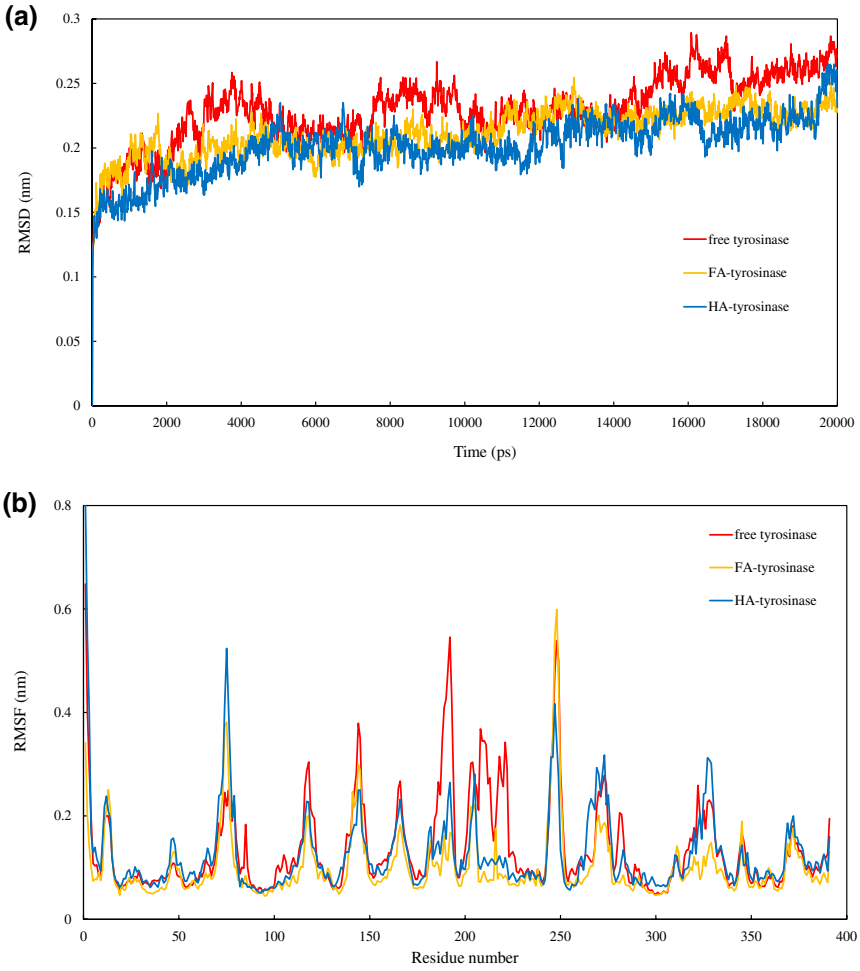

FIGURE 6 Findings of the MD simulations as a function of the simulation time. (a) the RMSD value of free tyrosinase, HA-tyrosinase, and FA-tyrosinase complexes. (b) the RMS fluctuation value of free tyrosinase and HA-tyrosinase, and FA-tyrosinase complexes.

demonstrated with brown string. Both inhibitors stretched into the hydrophobic pocket of tyrosinase. In the enzyme–inhibitor (HA or FA) complex, seven hydrogen bonds were detected between FA and the residues Glu-322 (bond length: 3.29 Å), Ala-323 (bond lengths: 2.94 and 3.13 Å), Cys-83 (bond length: 3.06 Å), His-85 (bond lengths: 2.88 and 3.25 Å), and Asn-81 (bond length: 3.18 Å). Five hydrogen bonds were detected between HA and the residues Ala-323 (bond length: 2.97 Å), Asn-81 (bond length: 3.08, 3.05, and 3.14 Å), Tyr-65 (bond length: 2.92 Å). For HA–tyrosinase interaction, 2 residues (Glu-322 and Ala-80) were included in hydrophobic interaction, however, for FA–tyrosinase interaction 3 residues (Thr-324, Thr-80, and Ala-80) were included in hydrophobic interaction.

RMSD is an influential factor employed to calculate the system equilibration through the simulation. The RMSF value offers a better insight into the structural fluctuations and enzyme flexibility (Farasat et al., 2020). The RMSD reports of the aforementioned complexes are demonstrated in Figure 6a, which reveals that the systems were stabilized nearly after 5 ns. In the last 5 ns of the simulation, the average values of RMSD of free tyrosinase, HA–tyrosinase, and FA–tyrosinase were 0.28, 0.26, and 0.25 nm, respectively. The RMSD differences between the substrate-tyrosinase and HA-tyrosinase or FA-tyrosinase were below 0.2 nm.

The value of RMSF offers a better knowledge about tyrosinase structural fluctuations as well as its flexibility (Farasat et al., 2020). The values of RMSF of substrate-tyrosinase, and HA-tyrosinase or FA-tyrosinase are indicated in Figure 6b. As the figure shows, each region for amino acid residues had equal RMSF values, except for residues 203–221. The substrate–tyrosinase complex fluctuation in the abovementioned residues varied from that in HA-tyrosinase or FA-tyrosinase. This implies that in the presence of HA or FA, the enzyme has less flexibility in the vicinity of these residues than in the existence of the substrate, which generated minor fluctuation and flexibility in tyrosinase.

4 | CONCLUSION

To the best of our knowledge, this research is the first that attempts to clarify the interactions of tyrosinase with FA or HA. The findings showed that FA and HA exhibited strong inhibition activity and these compounds inhibited the tyrosinase activity in a mixed-type manner. Thermodynamic analysis, CD spectroscopy analysis, and MD investigation indicated that the hydrophobic interaction was a major driving force in the HA-tyrosinase binding. However, in FA

and tyrosinase interaction, the hydrogen bond performs the main effect. HA could not damage the secondary structures of the tyrosinase significantly, however, it had a major impact on enzyme activity. In contrast, FA has a considerable influence on the secondary structure of tyrosinase and can cause the reduction of tyrosinase catalytic activity. Furthermore, one molecule of FA or HA combined with one molecule of tyrosinase and only one site in tyrosinase is reactive to FA or HA. Thus, both natural compounds could inhibit the activity of tyrosinase with different mechanisms. Previously, it has been shown that HA and FA have antioxidant properties and they can improve the quality of food via retarding lipid oxidation. Altogether, although further investigations are warranted to draw firm conclusions, HA and FA could be utilized in food industries not only as antioxidant agents but also as an accessible natural source for tyrosinase inhibition. These substances could be utilized in the soil or as a foliar spray, combined with chemicals/fertilizers, or by themselves.

ACKNOWLEDGMENTS

The technical support from the Institute of Biochemistry and Biophysics of Tehran University was appreciated.

FUNDING INFORMATION

This study obtained no certain grant and funding from any funding agency in the commercial, public, governmental, or not-for-profit sectors.

CONFLICT OF INTEREST

All authors declare no conflict of interest.

DATA AVAILABILITY STATEMENT

The data sets utilized and/or evaluated in the present research are accessible through the corresponding author.

COMPLIANCE WITH ETHICAL STANDARDS

This article does not include any experiments with animals performed or human participants by any of the authors.

ORCID

Azadeh Hekmat https://orcid.org/0000-0003-0123-1575
Kamahldin Haghbeen https://orcid.org/0000-0003-3011-5629

REFERENCES

Afifi, M. (2017). *Humic substances in organic fertilizers, properties and effectives* (1st ed.). Noor Publishing.

Ahmad, E., Rabbani, G., Zaidi, N., Singh, S., Rehan, M., Khan, M. M., & Ashraf, M. T. (2011). Stereo-selectivity of human serum albumin to enantiomeric and isoelectronic pollutants dissected by spectroscopy, calorimetry and bioinformatics. *PLoS One*, *6*(11), e26186. https://doi.org/10.1371/journal.pone.0026186

Albers, C. N., Banta, G. T., Jacobsen, O. S., & Hansen, P. E. (2008). Characterization and structural modelling of humic substances in field soil displaying significant differences from previously proposed structures. *European Journal of Soil Science*, *59*(4), 693–705. https://doi.org/10.1111/j.1365-2389.2008.01036.x

Anantharaman, A., Hemachandran, H., Priya, R. R., Sankari, M., Gopalakrishnan, M., Palanisami, N., & Siva, R. (2016). Inhibitory effect of apocarotenoids on the activity of tyrosinase: Multi-spectroscopic and docking studies. *Journal of Bioscience and Bioengineering*, *121*(1), 13–20. https://doi.org/10.1016/j.jbiosc.2015.05.007

Ashoka, S., Seetharamappa, J., Kandagal, P. B., & Shaikh, S. M. T. (2006). Investigation of the interaction between trazodone hydrochloride and bovine serum albumin. *Journal of Luminescence*, *121*(1), 179–186. https://doi.org/10.1016/j.jlumin.2005.12.001

Ashraf, Z., Rafiq, M., Seo, S.-Y., Kwon, K. S., & Babar, M. M. (2015). Kinetic and in silico studies of novel hydroxy-based thymol analogues as inhibitors of mushroom tyrosinase. *European Journal of Medicinal Chemistry*, *98*, 203–211. https://doi.org/10.1016/j.ejmech.2015.05.031

Athipornchai, A., Niyomtham, N., Pabuprapap, W., Ajavakom, V., Duca, M., Azoulay, S., & Suksamrarn, A. (2021). Potent tyrosinase inhibitory activity of curcuminoid analogues and inhibition kinetics studies. *Cosmetics*, *8*(2), 35. https://doi.org/10.3390/cosmetics8020035

Bondareva, L., & Kudryasheva, N. (2021). Direct and indirect detoxification effects of humic substances. *Agronomy*, *11*(2), 198. https://doi.org/10.3390/agronomy11020198

Burlingham, B. T., & Widlanski, T. S. (2003). An intuitive look at the relationship of Ki and IC50: A more general use for the Dixon plot. *Journal of Chemical Education*, *80*(2), 214. https://doi.org/10.1021/ed080p214

Chen, M.-J., Hung, C.-C., Chen, Y.-R., Lai, S.-T., & Chan, C.-F. (2016). Novel synthetic kojic acid-methimazole derivatives inhibit mushroom tyrosinase and melanogenesis. *Journal of Bioscience and Bioengineering*, *122*(6), 666–672. https://doi.org/10.1016/j.jbiosc.2016.06.002

Christl, I., Knicker, H., Kögel-Knabner, I., & Kretzschmar, R. (2008). Chemical heterogeneity of humic substances: Characterization of size fractions obtained by hollow-fibre ultrafiltration. *European Journal of Soil Science*, *51*, 617–625. https://doi.org/10.1111/j.1365-2389.2000.00352.x

Ding, G. B., Wu, G., Li, B., Yang, P., & Li, Z. (2019). High-yield expression in Escherichia coli, biophysical characterization, and biological evaluation of plant toxin gelonin. *3 Biotech*, *9*(1), 19. https://doi.org/10.1007/s13205-018-1559-6

Fan, M., Zhang, G., Pan, J., & Gong, D. (2017). An inhibition mechanism of dihydromyricetin on tyrosinase and the joint effects of vitamins B6, D3 or E. *Food & Function*, *8*(7), 2601–2610. https://doi.org/10.1039/C7FO00236J

Farasat, A., Ghorbani, M., Gheibi, N., & Shariatifar, H. (2020). In silico assessment of the inhibitory effect of four flavonoids (chrysin, naringin, quercetin, kaempferol) on tyrosinase activity using the MD simulation approach. *BioTechnologia. Journal of Biotechnology Computational Biology and Bionanotechnology*, *101*(3), 2601–2610. https://doi.org/10.1039/C7FO00236J

Gheibi, N., Ghorbani, M., Shariatifar, H., & Farasat, A. (2020). Effects of unsaturated fatty acids (arachidonic/oleic acids) on stability and structural properties of calprotectin using molecular docking and molecular dynamics simulation approach. *PLoS One*, *15*(3), e0230780. https://doi.org/10.1371/journal.pone.0230780

Gheibi, N., Taherkhani, N., Ahmadi, A., Haghbeen, K., & Ilghari, D. (2015). Characterization of inhibitory effects of the potential therapeutic inhibitors, benzoic acid and pyridine derivatives, on the monophenolase and diphenolase activities of tyrosinase. *Iranian Journal of Basic Medical Sciences*, *18*(2), 122–129. https://doi.org/10.22038/ijbms.2015.4012

Guan, Y.-F., Qian, C., Chen, W., Huang, B.-C., Wang, Y.-J., & Yu, H.-Q. (2018). Interaction between humic acid and protein in membrane fouling process: A spectroscopic insight. *Water Research*, *145*, 146–152. https://doi.org/10.1039/C7FO00236J

Hałdys, K., Goldeman, W., Jewgiński, M., Wolińska, E., Anger, N., Rossowska, J., & Latajka, R. (2018). Inhibitory properties of aromatic thiosemicarbazones on mushroom tyrosinase: Synthesis,

kinetic studies, molecular docking and effectiveness in melanogenesis inhibition. *Bioorganic Chemistry*, *81*, 577–586. https://doi.org/10.1016/j.bioorg.2018.09.003

Hanai, T., Koseki, A., Yoshikawa, R., Ueno, M., Kinoshita, T., & Homma, H. (2002). Prediction of human serum albumin–drug binding affinity without albumin. *Analytica Chimica Acta*, *454*, 101–108. https://doi.org/10.1016/S0003-2670(01)01515-X

Hassani, S., Gharechaei, B., Nikfard, S., Fazli, M., Gheibi, N., Hardré, R., & Haghbeen, K. (2018). New insight into the allosteric effect of l-tyrosine on mushroom tyrosinase during l-dopa production. *International Journal of Biological Macromolecules*, *114*, 821–829. https://doi.org/10.1039/C7FO00236J

Hekmat, A., Hatamie, S., & Bakhshi, E. (2021). Probing the effects of synthesized silver nanowire/reduced graphene oxide composites on the structure and esterase-like activity of human serum albumin and its impacts on human endometrial stem cells: A new platform in nanomedicine. *Nanomedicine Journal*, *8*(1), 42–56. https://doi.org/10.1039/C7FO00236J

Hekmat, A., Hatamie, S., & Saboury, A. A. (2022). The effects of synthesized silver nanowires on the structure and esterase-like activity of human serum albumin and their impacts on human endometrial stem cells. *Inorganic and Nano-Metal Chemistry*, *1-14*, 2601–2610. https://doi.org/10.1039/C7FO00236J

Hekmat, A., & Saboury, A. A. (2019). Structural effects of the Syntheticcobalt–manganese-zinc ferrite nanoparticles (co 0.3 Mn 0.2 Zn 0.5 Fe2 O 4 NPs) on DNA and its antiproliferative effect on T47D cells. *BioNanoScience*, *9*(4), 821–832. https://doi.org/10.1007/s12668-019-00657-5

Hridya, H., Amrita, A., Mohan, S., Gopalakrishnan, M., Dakshinamurthy, T. K., Doss, G. P., & Siva, R. (2016). Functionality study of santalin as tyrosinase inhibitor: A potential depigmentation agent. *International Journal of Biological Macromolecules*, *86*, 383–389. https://doi.org/10.1016/j.ijbiomac.2016.01.098

Hridya, H., Amrita, A., Sankari, M., Doss, C. G. P., Gopalakrishnan, M., Gopalakrishnan, C., & Siva, R. (2015). Inhibitory effect of brazilein on tyrosinase and melanin synthesis: Kinetics and in silico approach. *International Journal of Biological Macromolecules*, *81*, 228–234. https://doi.org/10.1177/1934578X20920055

Jacob, K. K., Prashob, P., & Chandramohanakumar, N. (2019). Humic substances as a potent biomaterials for therapeutic and drug delivery system-a review. *International Journal of Applied Pharmaceutics*, *11*, 1–4. https://doi.org/10.22159/ijap.2019v11i3.31421

Jamali, Z., Rezaei Behbehani, G., Zare, K., & Gheibi, N. (2019). Effect of chrysin omega-3 and 6 fatty acid esters on mushroom tyrosinase activity, stability, and structure. *Journal of Food Biochemistry*, *43*(3), e12728. https://doi.org/10.1111/jfbc.12728

Kinoshita, H., Kinoshita, M., Takahashi, A., Yuasa, S., & Fukuda, K. (2012). Effect of fulvic acid on ultraviolet induced skin aging: The effect of fulvic acid on fibroblasts and matrix metalloproteinase. *Nishinihon Journal of Dermatology*, *74*(4), 427–431. https://doi.org/10.2336/nishinihonhifu.74.427

Li, M., Chen, Y., Su, Y., Wan, R., & Zheng, X. (2016). Effect of fulvic acids with different characteristics on biological denitrification. *RSC Advances*, *6*(18), 14993–15001. https://doi.org/10.1039/C5RA26885K

Li, Y., Deng, B., Yang, S., Tian, H., & Sun, B. (2021). A colorimetric fluorescent probe for the detection of tyrosinase and its application for the food industry. *Journal of Photochemistry and Photobiology A: Chemistry*, *419*, 113458. https://doi.org/10.1016/j.jphotochem.2021.113458

Lindahl, E., Hess, B., & van der Spoel, D. (2001). GROMACS 3.0: A package for molecular simulation and trajectory analysis. *Molecular Modeling Annual*, *7*(8), 306–317. https://doi.org/10.1007/s008940100045

Liu, H.-J., Ji, S., Fan, Y.-Q., Yan, L., Yang, J.-M., Zhou, H.-M., & Wang, Y.-L. (2012). The effect of D-(−)-arabinose on tyrosinase: An integrated study using computational simulation and inhibition kinetics. *Enzyme Research*, *2012*, 1–10. https://doi.org/10.1155/2012/731427

Lu, Q., Chen, C., Zhao, S., Ge, F., & Liu, D. (2016). Investigation of the interaction between gallic acid and α-amylase by spectroscopy. *International Journal of Food Properties*, *19*(11), 2481–2494. https://doi.org/10.1080/10942912.2015.1059345

Moosavi-Movahedi, A., Golchin, A., Nazari, K., Chamani, J., Saboury, A., Bathaie, S., & Tangestani-Nejad, S. (2004). Microcalorimetry, energetics and binding studies of DNA–dimethyltin dichloride complexes. *Thermochimica Acta*, *414*(2), 233–241. https://doi.org/10.1016/j.tca.2004.01.007

Mu, Y., Li, L., & Hu, S.-Q. (2013). Molecular inhibitory mechanism of tricin on tyrosinase. *Spectrochimica Acta Part A: Molecular and Biomolecular Spectroscopy*, *107*, 235–240. https://doi.org/10.1016/j.saa.2013.01.058

Nanok, K., & Sansenya, S. (2020). α-Glucosidase, α-amylase, and tyrosinase inhibitory potential of capsaicin and dihydrocapsaicin. *Journal of Food Biochemistry*, *44*(1), e13099. https://doi.org/10.1111/jfbc.13099

Pashah, Z., Hekmat, A., & Hesami Tackallou, S. (2019). Structural effects of diamond nanoparticles and paclitaxel combination on calf thymus DNA. *Nucleosides, Nucleotides and Nucleic Acids*, *38*(4), 249–278. https://doi.org/10.1080/15257770.2018.1515440

Peña-Méndez, E. M., Havel, J., & Patočka, J. (2005). Humic substances-compounds of still unknown structure: Applications in agriculture, industry, environment, and biomedicine. *Journal of Applied Biomedicine*, *3*(1), 13–24. https://doi.org/10.32725/jab.2005.002

Rahman, S., Rehman, M. T., Rabbani, G., Khan, P., AlAjmi, M. F., Hassan, M., & Kim, J. (2019). Insight of the interaction between 2, 4-thiazolidinedione and human serum albumin: A spectroscopic, thermodynamic and molecular docking study. *International Journal of Molecular Sciences*, *20*(11), 2727. https://doi.org/10.3390/ijms20112727

Robinson, P. K. (2015). Enzymes: Principles and biotechnological applications. *Essays in Biochemistry*, *59*, 1–41. https://doi.org/10.1042/bse0590001

Sander, M., Tomaszewski, J. E., Madliger, M., & Schwarzenbach, R. P. (2012). Adsorption of insecticidal Cry1Ab protein to humic substances. 1. Experimental approach and mechanistic aspects. *Environmental Science & Technology*, *46*(18), 9923–9931. https://doi.org/10.1021/es3022478

Tan, K. H. (2014). *Humic matter in soil and the environment* (2nd ed.). CRC Press. https://doi.org/10.1201/b17037

Tan, W., Koopal, L., Weng, L., Van Riemsdijk, W., & Norde, W. (2008). Humic acid protein complexation. *Geochimica et Cosmochimica Acta*, *72*(8), 2090–2099. https://doi.org/10.1016/j.gca.2008.02.009

Tan, W. F., Koopal, L. K., & Norde, W. (2009). Interaction between humic acid and lysozyme, studied by dynamic light scattering and isothermal titration calorimetry. *Environmental Science & Technology*, *43*(3), 591–596. https://doi.org/10.1021/es802387u

Tomaszewski, J. E., Madliger, M., Pedersen, J. A., Schwarzenbach, R. P., & Sander, M. (2012). Adsorption of insecticidal Cry1Ab protein to humic substances. 2. Influence of humic and fulvic acid charge and polarity characteristics. *Environmental Science & Technology*, *46*(18), 9932–9940. https://doi.org/10.1021/es302248u

Uesugi, D., Hamada, H., Shimoda, K., Kubota, N., Ozaki, S.-I., & Nagatani, N. (2017). Synthesis, oxygen radical absorbance capacity, and tyrosinase inhibitory activity of glycosides of resveratrol, pterostilbene, and pinostilbene. *Bioscience, Biotechnology, and Biochemistry*, *81*(2), 226–230. https://doi.org/10.1080/09168451.2016.1240606

van Rensburg, C. E. (2015). The antiinflammatory properties of humic substances: A mini review. *Phytotherapy Research*, *29*(6), 791–795. https://doi.org/10.1002/ptr.5319

Wahyudi, I., Handayanto, E., Sykehfani, S., & Utomo, W. H. (2010). Humic and fulvic acids of gliricidia and tithonia composts for aluminium detoxification in an ultisol. *AGRIVITA, Journal of Agricultural Science*, *32*(3), 216–224. https://doi.org/10.17503/agrivita.v32i3.12

Yang, J., Chang, R., Ge, S., Zhao, M., Liang, C., Xiong, L., & Sun, Q. (2016). The inhibition effect of starch nanoparticles on tyrosinase activity

and its mechanism. *Food & Function*, *7*(12), 4804–4815. https://doi.org/10.17503/agrivita.v32i3.12

Yin, S.-J., Si, Y.-X., Chen, Y.-F., Qian, G.-Y., Lü, Z.-R., Oh, S., & Lee, D.-Y. (2011). Mixed-type inhibition of tyrosinase from agaricus bisporus by terephthalic acid: Computational simulations and kinetics. *The Protein Journal*, *30*(4), 273–280. https://doi.org/10.1007/s10930-011-9329-x

Yin, S.-J., Si, Y.-X., & Qian, G.-Y. (2011). Inhibitory effect of phthalic acid on tyrosinase: The mixed-type inhibition and docking simulations. *Enzyme Research*, *2011*, 1–7. https://doi.org/10.4061/2011/294724

You, S.-H., Yoon, M.-Y., & Moon, J.-S. (2021). Antioxidant and anti-inflammatory activity study of fulvic acid. *Journal of Natural Science, Biology and Medicine*, *12*(3), 285–289. https://doi.org/10.4103/jnsbm

Yu, Q., Fan, L., & Duan, Z. (2019). Five individual polyphenols as tyrosinase inhibitors: Inhibitory activity, synergistic effect, action mechanism, and molecular docking. *Food Chemistry*, *297*, 124910. https://doi.org/10.1016/j.foodchem.2019.05.184

Zhang, X., Zhai, H., Gao, R., Zhang, J., Zhang, Y., & Zheng, X. (2014). Study on the interaction between 4-thio-5-methyluridine and human serum albumin by spectroscopy and molecular modeling. *Spectrochimica Acta. Part A, Molecular and Biomolecular Spectroscopy*, *121*, 724–731. https://doi.org/10.1016/j.saa.2013.11.113

Zhou, L., Liu, W., Xiong, Z., Zou, L., Chen, J., Liu, J., & Zhong, J. (2016). Different modes of inhibition for organic acids on polyphenoloxidase. *Food Chemistry*, *199*, 439–446. https://doi.org/10.1016/j.foodchem.2015.12.034

Zolghadri, S., Bahrami, A., Hassan Khan, M. T., Munoz-Munoz, J., Garcia-Molina, F., Garcia-Canovas, F., & Saboury, A. A. (2019). A comprehensive review on tyrosinase inhibitors. *Journal of Enzyme Inhibition and Medicinal Chemistry*, *34*(1), 279–309. https://doi.org/10.1080/14756366.2018.1545767

How to cite this article: Taherkhani, N., Hekmat, A., Piri, H., & Haghbeen, K. (2022). Structural and inhibitory effects of fulvic and humic acids against tyrosinase. *Journal of Food Biochemistry*, 46(10), e14279. https://doi.org/10.1111/jfbc.14279